

Electron emission induced by fast heavy ions in a thin silicon crystal

F. Barrué,¹ M. Chevallier,¹ D. Dauvergne,¹ R. Kirsch,¹ J.-C. Poizat,¹ C. Ray,^{1,*} L. Adoui,² A. Cassimi,² H. Rothard,² M. Toulemonde,² C. Cohen,³ A. L'Hoir,³ D. Vernhet,³ C. Demonchy,⁴ L. Giot,⁴ W. Mittig,⁴ S. Pita,⁴ P. Roussel-Chomaz,⁴ and A. Billebaud⁵

¹*IPNL/IN2P3, Université Lyon I, 69622 Villeurbanne Cedex, France*

²*CIRIL/CEA-CNRS-ENSICAEN, BP 5133, 14070 Caen Cedex 05, France*

³*GPS, Universités Paris VI/VII, Campus Boucicaut, 140 rue de Lourmel, 75015 Paris, France*

⁴*GANIL/CEA-IN2P3, BP 5027, 14076 Caen, Cedex 05, France*

⁵*LPSC/IN2P3, 38026 Grenoble Cedex, France*

(Received 28 February 2004; published 9 September 2004)

We report observations of backward and forward electron emission by a thin silicon crystal target traversed by 29 MeV/u Pb⁵⁶⁺ incident ions. For each incident ion we have performed measurements of backward and forward electron emission, of the energy loss and of the charge state of the transmitted ion. The crystal target was traversed by incident ions either in random incidence or in axial alignment conditions. In both cases these correlated measurements bring original information on electron emission. In random conditions, using an incident ion species with a charge quite far from equilibrium, we observe correlations between backward and forward electron emission, that we understand when analyzing the associated charge exchange and energy-loss data. In channeling conditions, we added electron emission measurements to simultaneous energy-loss and charge state measurements (that are known to characterize quite precisely the type of trajectory of a projectile transmitted through a thin crystal). This allowed us to observe the reduced electron emission due to hyperchanneled ions, that interact mainly with target valence electrons, and also the enhanced electron emission due to projectiles entering the crystal very close to atomic strings.

DOI: 10.1103/PhysRevA.70.032902

PACS number(s): 34.50.Dy, 61.85.+p, 34.70.+e

Electron emission from solid surfaces under bombardment of fast charged projectiles is a direct consequence of the process of electronic energy loss by the projectiles. Ionizing collisions with target atoms produce primary electrons that may induce secondary electrons (cascade multiplication). Primary and secondary electrons may leave the solid if they happen to reach the surface with the minimum required energy. The energy spectrum of emitted electrons is essentially a continuum, extending up to around E_M , the maximum energy that can be transferred during a close encounter with an electron at rest.

If the target is a single crystal, electron emission yields are expected to be modified by channeling effects. Most channeling studies have been performed using thick targets bombarded by low-energy heavy ions [1], and showed a strong reduction of electron yields in alignment conditions. Zhao *et al.* [2] have observed channeling effects on electron emission by 1-MeV protons traversing a thin $\langle 100 \rangle$ silicon crystal and measured yields equal to ~ 0.6 times the yields measured in random conditions, both for backward and forward emission. Recent channeling studies, performed on thick crystals with faster heavy projectiles by Kudo and co-workers [3–5], were devoted to the spectrometry of high-energy electrons and the main observed feature is the strong reduction of electron yields above E_M , those electrons resulting from binary interactions with fast inner-shell target elec-

trons. These latter experiments were not dealing with low-energy electrons, which, however, represent by far the largest part of the emitted electrons. Yet they suggest that channeling effects vanish for low-energy electrons and that the orientation effects on the mean electron multiplicity should be small. However, even if there were no overall effects on the electron multiplicity, the electron emission for each incident projectile is expected to depend on its particular trajectory in the crystal, a feature that is one of the goals of this paper. We present here the most striking results of this original experimental study, in which we have performed event-by-event measurements of secondary electron emission (mainly low-energy electron multiplicities) under impact of fast heavy ions in axial and planar alignment conditions as well as for random orientation of a thin silicon crystal: for each heavy ion sent onto the crystal we measured simultaneously the electron multiplicities of backward and forward emissions (from the entrance and the emergence surfaces, respectively), as well as the charge state and the energy loss of the transmitted ions.

The incident projectile (species and energy) was chosen to be far from charge equilibrium in random conditions. In our experiment carries much more electrons than in its charge state at equilibrium. Then the dominant charge exchange process in the target is electron loss. Such a situation is quite useful both in random conditions, as we will see, and in alignment conditions because it allows us to characterize rather precisely the trajectory of projectiles as their energy loss and their charge state at emergence are tightly connected

*Electronic address: c.ray@ipnl.in2p3.fr

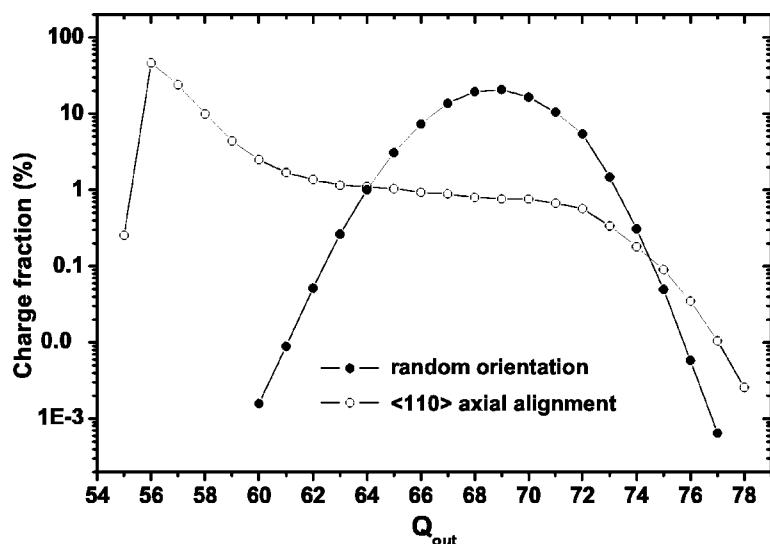


FIG. 1. Charge-state distributions for 29-MeV/u Pb^{56+} incident ions transmitted after a path of $1.12 \mu\text{m}$ in silicon, in random conditions and for $\langle 110 \rangle$ alignment.

to their transverse energy¹ [6,7]. Although this work was initially devoted to crystal orientation effects on electron emission, the preliminary study performed in random conditions appeared to bring valuable information and will be presented in detail. As for experiments in alignment conditions, we present the most interesting cases of axial alignment: the case of hyperchanneled projectiles that experience a very low electron density throughout the crystal, and the case of near-zero impact parameter projectiles that enter the crystal in regions of high atomic and electronic densities.

The experiment was performed at the GANIL (Caen) facility. A tightly collimated beam of 29-MeV/u $^{208}\text{Pb}^{56+}$ ions was sent in the SPEG beam line onto a $0.79\text{-}\mu\text{m}$ -thick $\langle 100 \rangle$ silicon single crystal held by a two-axis goniometer. The crystal was chosen thin enough to induce a negligible transverse energy increase during the target traversal in alignment conditions. The crystal was tilted at 45° in such a way that the beam could be oriented along various directions around the $\langle 110 \rangle$ axis. The tilt angle was needed for electron detection, using the technique introduced by Yamazaki and Kuroki [8], as well as the setting of the crystal at a negative potential $-V_0$ ($V_0 \sim 10$ kV). A silicon detector, Si-in, located at 135° to the beam direction and then facing the entrance surface of the crystal, was grounded in order to attract all low-energy

electrons emitted in any direction. A second grounded silicon detector, Si-out, located at 45° to the beam direction and facing the emergence surface of the crystal detected forward emitted electrons. In order to avoid pile-up problems the incident beam intensity was kept below 10^4 particles/s. For each detector, calibrated with a ^{241}Am source, and for each projectile, the value n of the multiplicity is deduced from the theoretical signal amplitude neV_0 (e being the elementary charge). However, it is known that a fraction of electrons ($\sim 15\%$ for $V_0 = 10$ kV) are backscattered out of the detector [9]. As a consequence the measured value of multiplicities are somewhat below the real values. This is of minor importance when one compares multiplicities obtain with a given detector, but must be kept in mind when one compares backward and forward emissions.

The projectiles emerging from the crystal were charge and energy analyzed in the high-resolution magnetic spectrometer of the SPEG beam line, in which the ions were detected by a drift chamber. The measured full width at half maximum (FWHM) of the direct beam peak was 0.3 MeV. This energy resolution allows us to measure the energy losses in this thin crystal (the energy loss in random conditions was about 15 MeV for an effective path of $1.12 \mu\text{m}$). Each event was triggered by the detection of a transmitted ion, and contained information on the corresponding charge state and energy loss, together with the multiplicities of low-energy electrons emitted at incidence and emergence. This provides detailed insight into the dependence of secondary electron emission upon entrance or emergence conditions. We first present the results obtained for random incidence conditions, that not only will be needed as a reference for the channeling study to follow, but also happen to contain interesting features that link electron emission, energy loss, and charge exchange of fast heavy ions in solids.

In Fig. 1 we show the charge distributions of transmitted ions for a random crystal orientation. This charge distribution appears Gaussian like and centered around a mean charge of 68.5 , much higher than the charge state at incidence. According to measurements performed with Pb ions of the same energy in aluminum targets [10], that yielded an equilibrated mean charge of 71.5 for target thicknesses above $\sim 4 \mu\text{m}$,

¹In conditions of alignment with an axial or a planar direction, the transverse energy of a projectile of given charge and of energy E is the sum of its potential energy in the axial or planar continuum potential and of its transverse kinetic energy $E\phi^2$, where ϕ is the instantaneous angle between the projectile trajectory and the axial or planar direction. The transverse energy of a projectile can be considered to be constant during the traversal of a thin crystal and is then determined by the entrance conditions of the projectile into the crystal (i.e., the distance to the nearest atomic string or plane, and the angle between the direction of incidence and the axial or planar direction). The smallest transverse energies correspond to the best channeled projectiles (call hyperchanneled in the axial case when they are confined to one axial channel). Projectiles that enter the crystal at zero degree and very close to an atomic string or plane have a so-called critical transverse energy that is equal to the height of the continuum potential barrier.

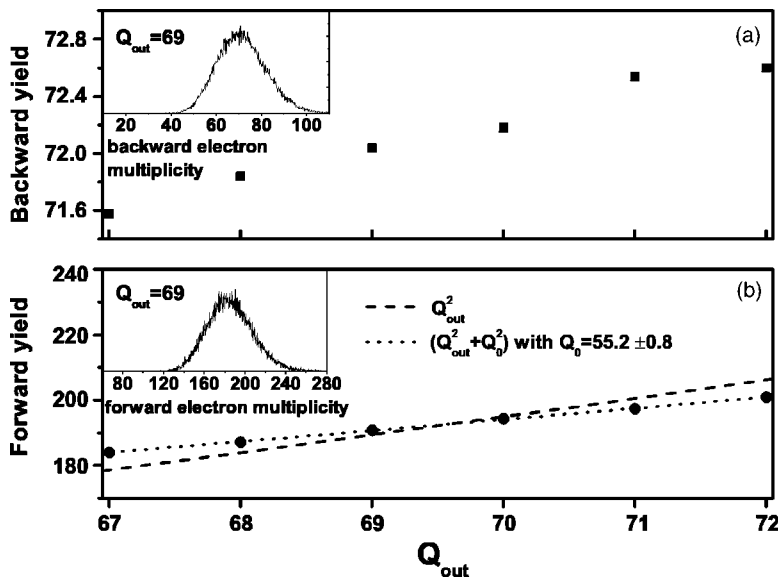


FIG. 2. Random crystal orientation: Q_{out} dependence of (a) backward and (b) forward electron yields (expressed in number of electrons per projectile). Insets show electron multiplicity distributions for $Q_{out}=69$. See text for explanation of fits.

the charge equilibrium in silicon should be around 71. Equilibrium is still not reached over the 1.12- μm path in the present distribution.

Nonequilibrium also clearly appears in electron emission measurements, as illustrated in Fig. 2, both for backward [Fig. 2(a)] and forward [Fig. 2(b)] emissions. In the insets we show, as examples, the amplitude spectra given by the detectors Si-in and Si-out in coincidence with the detection of transmitted 69+ ions. The yield associated to each spectrum is the mean number of electrons emitted per incident projectile. The electron yields are of about 70 and 190 electrons for the backward and the forward emission, respectively. These values (and their ratio), are compatible with available experimental values obtained in other conditions [11]. The multiplicity distributions appear slightly skew; the tail on the high multiplicity side is known to be due to the rare violent binary collisions with target electrons (δ electrons) that may induce large electron cascades. The results presented in Fig. 2 show that both backward and forward electron yields depend on the charge state at emergence Q_{out} . In Fig. 2(a), the very weak but significant increase with Q_{out} of the backward emission looks rather surprising since backward emission is essentially composed of low-energy electrons that are expected to originate from a few tens of angstroms, i.e., from a depth much smaller than the target thickness. The observed increase can be understood if considering that charge state equilibrium is not reached at emergence: schematically, 56+ incident ions steadily increase their charge state up to Q_{out} . Then, on the average, their charge-state increase in the entrance region is larger for higher values of Q_{out} . As a consequence the energy loss in this region (due to the dependence of energy loss on the ion charge) and thus the backward emission are also larger for higher values of Q_{out} . Moreover, this weak Q_{out} dependence may also be partially due to the contribution of the electrons removed from the projectiles in the same region.

As for forward emission [Fig. 2(b)], a stronger increase of the electron yield is observed when Q_{out} increases. As shown on the figure the yield does not follow a law in Q_{out}^2 but a law in $(Q_{out}^2 + Q_0^2)$, with a Q_0 value (55.2) that is close enough to

the initial charge state to allow us to conclude that the whole target (or at least a very large fraction of it) contributes here to the forward electron emission. This is compatible with previous studies devoted to the dependence on the target thickness of electron emission induced by heavy ions in carbon targets [11]. Such observations do indeed demonstrate unambiguously that forward electron emission does not originate only from the vicinity of the exit surface.

The same linear dependence on $(Q_{out}^2 + Q_0^2)$ is observed for the mean energy loss of transmitted ions. However the most interesting feature appears when examining energy loss spectra, as illustrated by Fig. 3. Here we show as an example the energy spectrum of ions transmitted with $Q_{out}=69$ [Fig. 3(b)]. The FWHM of this Gaussian-like peak is about 1.3 MeV, which is almost twice the width expected from straggling effects due to collision statistics. This broadening must be attributed to charge changing processes, and more specifically to the fluctuations of the depths at which successive electron loss events take place in the target. This is also the origin of the effect illustrated in Fig. 3(a), where we give backward and forward electron yields associated with the transmission of ions with $Q_{out}=69$ that have lost various amounts of energy as indicated on the energy-loss spectrum of Fig. 3(b). Both backward and forward electron yields are seen to increase with energy-loss, a dependence that is observed also for the other Q_{out} values. The reason is that, for a given Q_{out} value, projectiles that lose more energy must have had a higher mean charge state inside the target and then emit more electrons, both backwards and forwards. An interesting consequence of the above effect is that we do observe a correlation between backward and forward electron emissions for a given Q_{out} value. Such a correlation had been already observed some years ago by Yamazaki *et al.* [12] with 1.8 MeV-Ar ions bombarding thin carbon foils, and tentatively explained by the authors as resulting from the conversion of bulk plasmons into electron-hole pairs. In spite of the fact that the transmitted Ar ions in Ref. [12] were charge equilibrated (contrary to the transmitted Pb ions in the present experiment), charge changing and energy straggling could well offer an alternative explanation for the correlations they observed.

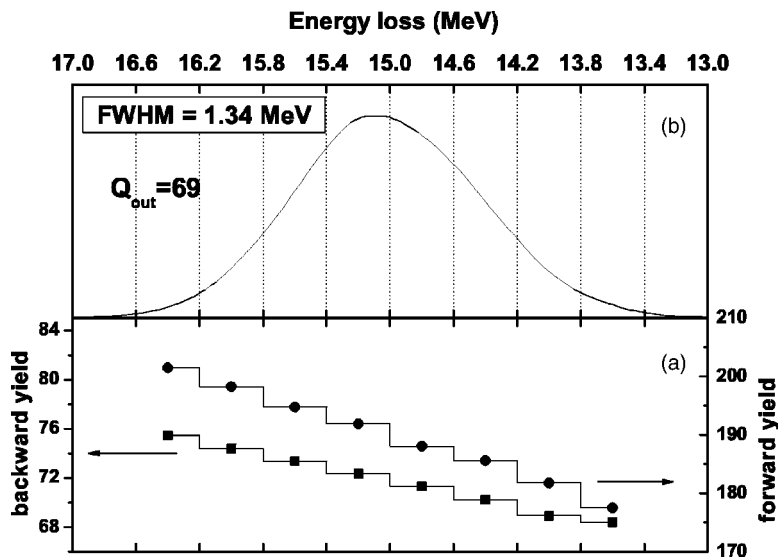


FIG. 3. Random crystal orientation, for $Q_{out}=69$: (a) variations of backward (full square) and forward (full circle) electron yields (expressed in number of electrons per projectile) with the energy loss in the target, the spectrum of which is given in (b).

The study of electron emission for incidence directions close to axial or planar orientations, combined with energy and charge measurements, leads to more specific conclusions, thanks to the precise knowledge of the trajectories throughout the crystal. Here we discuss only features observed in axial alignment. In Fig. 1 we show the charge distribution of the projectiles transmitted in conditions of alignment with the $\langle 110 \rangle$ axial direction. The broadness of the distribution reflects the variety of the entrance conditions of the projectiles into the crystal. The most abundant is the fraction 56+ (about 50%) due to well channeled particles that entered the crystal far from atomic strings: they stay frozen in their initial charge state because they avoid nuclear impact ionization and experience only low electron densities, which reduces electron loss drastically (note that a small fraction of them emerge as 55+ ions, that we ascribe to a mechanical capture event in one of the two thin amorphous layers on the crystal surfaces).

The increasing charges correspond to ions with increasing transverse energies that experience increasing electron densities and thus have increasing electron impact ionization rates. The high charge state side corresponds to unchanneled projectiles that entered the crystal close to an atomic string and that can lose (and capture) electrons in binary collisions with target atoms. Contrary to previous channeling studies using also fast incident heavy ions with many electrons [6,7], where the unchanneled component mimics the random charge distribution, this component here extends not only beyond the observed random orientation distribution but also beyond its expected position at charge equilibrium. This result shows that charge exchange processes are enhanced for projectiles that spend part of their path close to atomic rows, where nuclei and electron densities are large. The main result, however, is that electron loss is enhanced more than electron capture. We attribute this to a “superdensity” effect, that results from the high collision frequency near the atomic rows where the charge exchange events take place. Analogous to the well known density effect [13] responsible for the differences in the charge state distributions of slower (a few MeV) heavy ions after traversal of gas and solid targets, this

orientation effect is based on the strong reduction, with respect to random conditions, of the mean time interval (5×10^{-18} s) between two successive collisions of the projectiles with target atoms in atomic rows. This may increase the mean electronic excitation of projectile bound electrons and then increase their probability to be lost. This effect is observable here because of the thinness of the crystal, that leaves no time to a projectile of high transverse energy to change its transverse energy and then to explore uniformly the transverse space. We will describe these effects in more detail in a forthcoming paper.

The electron emission yields for $\langle 110 \rangle$ alignment depend strongly on the Q_{out} value, i.e., on the transverse energy of the projectiles in the crystal. They are smaller than in random conditions for well channeled projectiles and much higher for high transverse energy projectiles emerging in a high charge state. However, the overall effect of $\langle 110 \rangle$ alignment is rather small, since the yields, integrated over all transmitted ions, are measured to be 0.9 and 0.6 for backward and forward emission, respectively, in units of the total yield measured for a random crystal orientation. Parts of our results are given in Fig. 4, where we show backward and forward electron multiplicity distributions and energy-loss spectra, obtained for transmitted ions of Q_{out} 56 and 72, respectively. For comparison the spectra obtained in random conditions for $Q_{out}=72$ are also shown.

First we consider energy-loss: the measured energy loss of well channeled projectiles frozen in their initial charge state 56 is much smaller than the random energy-loss. There are two reasons for that: the first one is the well-known property of channeled projectiles to encounter lower target electron densities than projectiles traveling in random conditions. The second reason is the Q^2 dependence of energy-loss: other things being equal, 56+ ions lose less energy than ions increasing their charge in the target from 56 to 72. In order to determine the reduction factor of the energy-loss rate due to the specific trajectories of channeled ions, it is necessary to remove the charge dependence of energy loss from measured values, what we did using the $(Q_0^2 + Q_{out}^2)$ law discussed above. Then we obtain the “charge-corrected” energy-loss

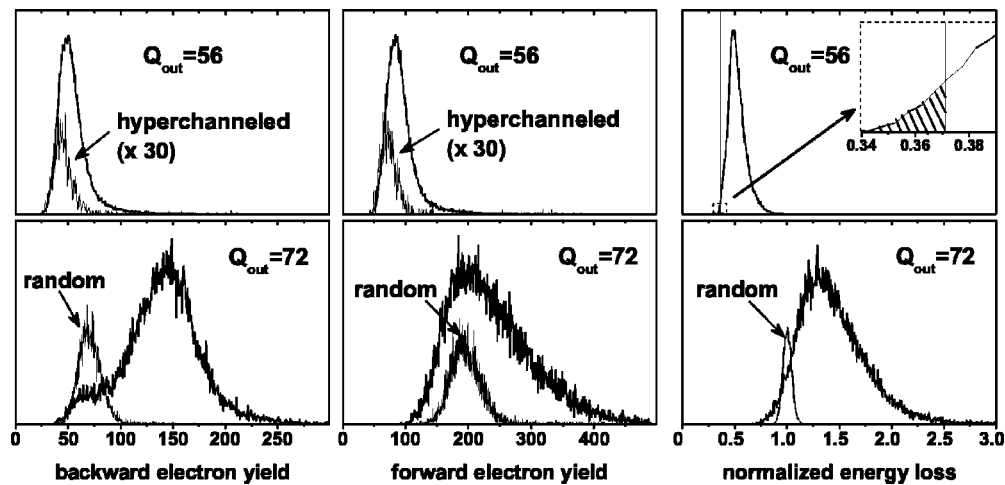


FIG. 4. From left to right: distributions of backward and forward electron multiplicities and corrected energy loss spectra (see text) associated with ions incident along the $\langle 110 \rangle$ direction and transmitted with charge states 56 (top) and 72 (bottom), respectively. For 56+ ions the electron multiplicity distributions of hyperchanneled ions (with the most reduced energy loss, see top-right inset) are shown. For 72+ ions the spectra obtained in random conditions are also shown.

spectra of Fig. 4, where “corrected” energy-losses are expressed in units of the mean random energy loss. Whereas the mean reduction factor is $\sim 50\%$ for 56+ ions, the reduction factor for hyperchanneled ions that lose the smallest amount of energy (see the enlargement the spectrum in the inset of Fig. 4) is about 0.35, in agreement with a wealth of published data, the most often obtained with lighter bare ions.

On the other side, the 72+ ions transmitted in axial alignment conditions are nonchanneled projectiles that entered the crystal very close to a string of atoms, where the energy loss rate is very large (Vickridge *et al.* [14] have measured an enhancement of ~ 8 for the energy loss of MeV protons in $\langle 110 \rangle$ atomic strings of an aluminum crystal). In the broad energy-loss spectrum of Fig. 4, the mean value is 1.45 times the energy loss of 72+ projectiles transmitted in random conditions, and the enhancement factor is seen to reach more than 2.5 for some projectiles. Monte Carlo simulations have shown that 29 MeV/u Pb projectiles entering along an $\langle 110 \rangle$ atomic string of silicon at zero impact parameter leave the string (i.e., depart from the string by more than the vibration amplitude of Si atoms) after ~ 500 Å on the average. A rough estimate shows that the factor 1.45 may result from an energy-loss enhancement of ~ 10 over the first 500 Å associated with a “random” energy loss in the rest of the crystal. In the same way the factor 2.5 may result from the same enhancement of ~ 10 over the first 500 Å, and over the ~ 1000 Å length of a second close interaction with an atomic string deeper in the crystal.

As for electron emission, we first consider the case of 56+ ions that represent about 50% of the transmitted beam. The backward and forward emission yields associated with frozen 56+ emergent projectiles are 55 and 92, respectively, i.e., about 0.75 and 0.5 times the yields observed in random conditions. This illustrates clearly the fact that electron emission is tightly connected to energy loss. Qualitatively, the reduction of close encounter ion-electron collisions (which, on the average, produce forward directed electron cascades)

affects the forward emission more than the backward emission. We also show, in Fig. 4, the multiplicity distributions associated with the transmitted 56+ ions of the so-called leading edge (shaded part of the energy loss spectrum), that represent about 5×10^{-3} of the transmitted beam. They are then the very best hyperchanneled projectiles and sample a very small target electron density. The associated backward and forward yields (47 and $76e^-$, respectively) are only slightly lower than the yields associated with the whole 56+ charge fraction that samples a much higher electron density in the crystal (the ratio of the above electron densities is larger than 5). This demonstrates that electron emission is not only dependent on the local electron density but that distant collisions must also be considered, as for energy-loss.

In particular, one can expect that collective excitation of the target electron gas plays a dominant role in electron emission by hyperchanneled projectiles, as it does for energy-loss. If this process were exclusive, electron emission following plasmon decay should have the property of backward-forward symmetry. As our experimental geometry and the frozen charge of hyperchanneled projectiles respect this symmetry, one should measure equal yields for backward and forward electron emission in this case. We do not observe this (even if — as mentioned above — one must be careful in comparing backward and forward yields) but rather measure a larger forward emission, even if the ratio of the forward yield over the backward yield is somewhat smaller than in random conditions. The persistence of this asymmetry between backward and forward emission by hyperchanneled projectiles can be understood as follows: for those highly charged projectiles, binary collisions with large energy transfers may involve target electrons far from their trajectories [6,15], i.e., far from the center of the $\langle 110 \rangle$ channel. Moreover, the electron emission from the thin amorphous surface layers may bring a small contribution to the observed asymmetry.

Comparing quantitatively the yields obtained for hyperchanneled projectile to yields obtained in random condition is a difficult task that would require more experimental work.

The reason is mainly that the energy distribution of electrons set in motion following plasmon decay is probably quite different from the distribution resulting from binary collisions (particularly for backward emission). As a consequence the regions of the crystal involved in electron emission must be different in the two cases. For forward emission the situation is further complicated by its dependence upon the target thickness and the ion charge state at emergence.

As for electron emission associated with $72+$ emergent ions, the multiplicity distributions shown on Fig. 4 are very broad, with yields of 142 and 241 e^- for backward and forward emission, respectively. The increase with respect to random values associated with the same emergent charge $72+$ is particularly spectacular for backward emission, which is enhanced by a factor ~ 2 on the average. The enhancement reaches values up to 3, that are associated with projectiles that enter the crystal near a string of atoms and that have, as discussed above, a very high-energy-loss rate when they enter the crystal. The forward emission is also significantly enhanced with respect to random conditions, but less than backward emission. This was expected since we already know that the whole target contributes to forward emission. This is also the reason for which the distribution of forward emission multiplicity and energy loss are quite similar. However, it must be noted that the enhancement of the most probable energy-loss, with respect to the random case, is larger than the most probable forward emission multiplicity. This shows that the contribution of the projectile entrance region to forward emission is significantly attenuated for the 1- μm -thick crystal target used in our experiment. Moreover,

as for energy-loss, the high multiplicity tail corresponds to projectiles that suffer a second close interaction with an atomic string in the crystal bulk.

To conclude, we have observed electron emission from a thin silicon crystal under impact of fast Pb ions. We have clearly shown how electron emission induced by a fast heavy ion in a thin solid target is correlated to its energy loss and to its charge state at emergence, both for a random orientation of the crystal and for axial alignment conditions. In particular we have performed an observation of electron emission by hyperchanneled projectiles and by projectiles entering a crystal close to an atomic string. We show in particular which electron emission by hyperchanneled projectiles is strongly reduced with respect to random conditions, even if the specific emission resulting from plasma excitation has not been fully isolated. More work should be needed for this, that could involve lighter incident species or varied crystal thicknesses and that should shed additional light on the electron excitation processes in solids.

Moreover, our results show that electron emission, and specially backward emission, is very sensitive to the type of trajectory of the projectile in alignment conditions, and may then provide a precise way of determining the entrance conditions of projectiles in a crystal.

We wish to thank J. Chevallier for supplying us with the silicon crystal and the GANIL staff for providing us high quality beams. We specially thank P. Gangnan and J.-F. Libin for their strong support in operating the SPEG beam line.

-
- [1] N. Benazeth, Nucl. Instrum. Methods Phys. Res. **194**, 405 (1982).
 - [2] Z. Y. Zhao *et al.*, Nucl. Instrum. Methods Phys. Res. B **99**, 30 (1995).
 - [3] H. Kudo, K. Shima, S. Seki, K. Takita, K. Masuda, K. Murakami, and T. Ipposhi, Phys. Rev. B **38**, 44 (1988).
 - [4] H. Kudo, K. Shima, K. Masuda, and S. Seki, Phys. Rev. B **43**, 12729 (1991).
 - [5] H. Kudo, K. Shima, S. Seki, and T. Ishihara, Phys. Rev. B **43**, 12736 (1991).
 - [6] A. L'Hoir *et al.*, Nucl. Instrum. Methods Phys. Res. B **48**, 145 (1990).
 - [7] D. Dauvergne *et al.*, Phys. Rev. A **59**, 2813 (1999).
 - [8] Y. Yamazaki and K. Kuroki, Nucl. Instrum. Methods Phys. Res. A **262**, 118 (1987).
 - [9] A. Billebaud, M. Fallavier, R. Kirsch, J.-C. Poizat, J. Remilieux, and Z. Vidović, Phys. Rev. A **55**, 1124 (1997).
 - [10] A. Leon *et al.*, At. Data Nucl. Data Tables **69**, 217 (1998).
 - [11] M. Jung, H. Rothard, B. Gervais, J.-P. Grandin, A. Clouvas, and R. Wünsch, Phys. Rev. A **54**, 4153 (1996).
 - [12] Y. Yamazaki *et al.*, Phys. Rev. Lett. **70**, 2702 (1993).
 - [13] H. D. Betz, Rev. Mod. Phys. **44**, 465 (1972).
 - [14] I. Vickridge, A. L'Hoir, J. Gyulai, C. Cohen, and F. Abel, Europhys. Lett. **13**, 635 (1990).
 - [15] J. U. Andersen *et al.*, Phys. Rev. A **54**, 624 (1996).